

A Structural Model For Simulating the Mechanical Response of Fingertip to Tactile Stimuli

R. Khodambashi ^a

*M.Sc. student, Amirkabir University
of Technology Tehran, Iran
rkhodam@aut.ac.ir*

S. Najarian ^a

*Professor, Amirkabir University
of Technology Tehran, Iran
najarian@bme.aut.ac.ir*

A. T. Golpaygani ^a

*Ph.D. student, Amirkabir University
of Technology Tehran, Iran
tavakoli.golpa@aut.ac.ir*

A. A. Dehkordi ^b

*M.Sc. student, Amirkabir University
of Technology Tehran, Iran
abdi_dehkordi@aut.ac.ir*

^a Artificial Tactile Sensing and Robotic Surgery Lab, Faculty of Biomedical Engineering

^b Faculty of Mechanical Engineering

Abstract

Response of the mechanoreceptors underlying the skin is greatly affected by its mechanical properties. Knowledge of this response is essential in designing artificial tactile devices such as minimally invasive tools and tactile displays. The purpose of present research is to simulate the biomechanics of tactile sensation during indentation tests. A two-dimensional finite element model has been used for the analysis incorporating the essential anatomical structures of a finger (i.e., skin, subcutaneous tissue, bone, and nail). The skin and subcutaneous tissue are assumed to be hyperelastic and viscoelastic. We obtained the stress, strain and deformation fields in indentation tests. It was noted that the skin away from the indenter was experiencing considerable amount of strain energy density. Also, the response of SAI afferents could be predicted from the proposed model. These results were in agreement with the results mentioned in other published experimental data.

Keywords: Finite element model, Tactile sensation, Hyperelastic materials.

Introduction

In most studies in which the properties of cutaneous afferents have been investigated, the stimuli were confined to the classical receptive field. Punctuate probes indenting or vibrating into the skin of either humans or experimental animals were used to define the temporal or frequency characteristics of the afferents [1,2]. The spatial characteristics of their receptive fields were delineated by varying the position of the stimuli on the skin [3-7]. These initial studies of the receptive field established the differences in properties between the four classes of afferents that innervate human glabrous skin: the slowly adapting type I and type II afferents (SAIs and SAIIIs) and the fast adapting type I and type II afferents (FAIs and FAIIIs); for review see [8,9].

Skin indentation is encountered while performing several activities such as interacting with a virtual world through a tactile display. Some categories of tactile displays are

based on presenting an array of vibrating pins to the index finger and thus conveying some information about texture of the virtual surface [10-13].

A fingertip is composed of skin layers (epidermis and dermis), subcutaneous tissue, arterial bone, and nail (Figure 1). The epidermis, the outermost layer of the skin, consists of primarily protective horny structures, such as stratum corneum. The dermis, a fibrous layer supporting the epidermis, contains numerous mechanoreceptors which have been classified into four types. The subcutaneous tissue is a fat layer which primarily consists of lipocytes. The matrix of the subcutaneous tissue contains approximately 60–72% fluid in volume.

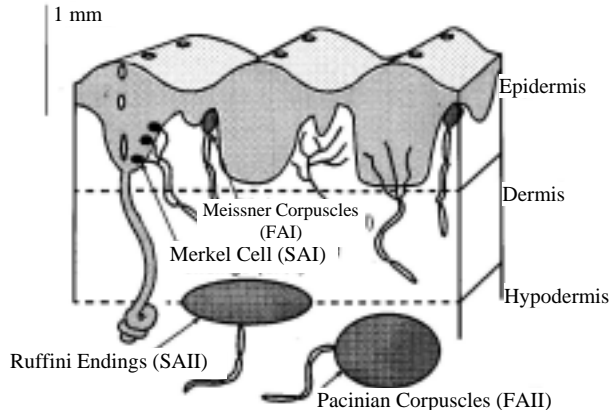


Figure 1: Cross-section of the skin showing its three layers along with the most important mechanoreceptors.

Mechanics of the skin and subcutaneous tissue is as central to the sense of touch as optics of the eye is to vision and acoustics of the ear to hearing. Biological tactile sensors found in the skin can simultaneously detect contact force, hardness, temperature, and surface roughness for multimodal, comprehensive evaluation of the contact object. To gain such information in real-time, the human fingertip uses its specialized structures such

as fast responding Meissner's (FAIs) and Pacinian corpuscles (FAIIs) for sensing vibration and texture and slow Ruffini endings (SAIs) and Merkel's discs (SAIIs) for sensing deformation. The relationship between these loads and the resulting stresses and strains at the mechanoreceptive nerve terminal within the skin plays fundamental role in the neural coding of tactile information. Understanding the principles of this coding is helpful in the design of artificial tactile systems which are gaining increasing application in different fields such as robotics and minimally invasive surgery [14].

Bisley et al. [15] recorded the responses from slowly adapting type I primary afferent fibers (SAIs) innervating the sides and end of the distal segment of the stimulated finger. They observed that although these afferents had receptive field centers that were remote from the stimulus, their responses were substantial and that increasing the curvature of the stimulus resulted in an increased response for most afferents. They analyzed the previously proposed models such as waterbed model of Srinivasan [16] and stated that since these models cannot predict their observations properly, there is a need for realistic models of the finger that will explain the distribution of stresses and strains over the entire skin surface in response to tactile stimuli.

In order to aid the design of tactile displays, we have analyzed the mechanical response of the fingertip to a tactile stimulus through finite element modeling. This stimulus is a rectangular bar with a rounded tip which simulates the indenter in an indentation test. The predicted mechanoreceptor response obtained from this model is compared with published experimental result.

Materials and Methods

1-Finite element model

A 2D finite element (FE) model of the fingertip is used for the analysis, as shown in Figure 2. The dimensions of the fingertip are assumed to be representative of the index finger of a male subject. The fingertip is assumed to be composed of a skin layer (representing epidermis and dermis), subcutaneous tissue, bone, and nail. The skin is assumed to have a thickness of 0.8 mm. The cross-sections of the fingertip and the bone are assumed to be elliptical and the tissue thickness is considered to be asymmetric about the bone.

The nail was fixed at its three upper nodes as in most experiments which fix the finger on a table for indentation test. The contact between the bone and subcutaneous tissue and between the nail and skin are assumed to be frictionless without any separation. Mapped meshing technique was used to mesh the model with a total number of 1065 two dimensional plane strain elements. An indenter was modeled to deform the skin surface of the fingertip. The indenter was modeled as a rectangular steel bar with rounded tip and was assumed to touch the skin surface without initial compression. The indenter was given different displacements in different time intervals and distribution of stress and strain

developed in the fingertip were obtained both as a function of both location and time. A typical loading curve has been plotted in Figure 3.

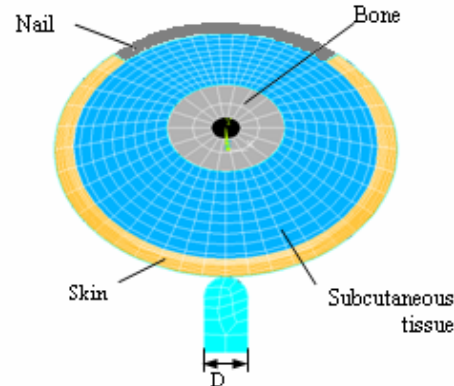


Figure 2: Finite element model of fingertip showing essential anatomical structures of a finger. The indenter diameter D was varied (0.1, 0.2, 2 and 4 mm) and its effect on stress and strain fields was studied.

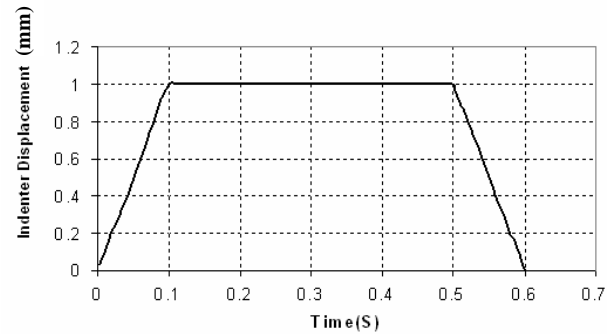


Figure 3: Displacement of the indenter as a function of time.

2- Material properties

The Young's moduli of the bone and nail were assumed, according to the published experimental data [17], to be 17.0 GPa and 170.0 MPa, respectively; while Poisson's ratio was assumed to be 0.30 for both. The material parameters of the skin and subcutaneous tissues used in the present simulations were determined based on the published experimental data [18], as in Table 1 in Appendix B. Constitutive equations for skin and subcutaneous tissue are given in Appendix A.

Results

The indenter was modeled to deform the skin surface of the fingertip by an amount of h within a ramping period of t , as shown in Figure 3. Two sets of finite element analyses were performed to study the mechanics of tactile sensation of the fingertip. In the first set, the indenter was given a displacement of $h = 1\text{mm}$ in a time of $t = 1\text{s}$. The displacement, stress and strain fields within the soft tissue at the state of maximum depression

$(t = 1 \text{ s})$ were obtained. The displacement contours are plotted in Figure 4.

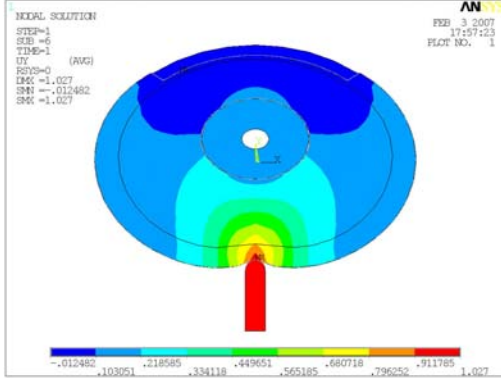


Figure 4: Distribution of displacement in y direction at $t = 1\text{s}$ and indenter diameter of 1mm .

It is seen that the displacement at the point of application of load is maximum and gradually decreases with increasing the distance from the load. Distribution of xy shear strain (e_{12}) at $t = 1\text{s}$ is shown in Figure 5. It can be seen that in addition to the contact region, other portions of the fingertip are also experiencing considerable shear strain.

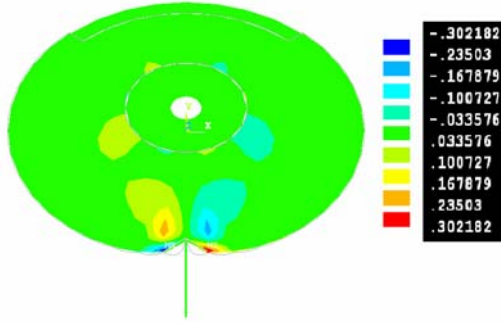


Figure 5: xy shear strain (e_{12}) at $t = 1\text{s}$ and indenter diameter of 0.1 mm .

Figure 6 shows the x component of strain (e_1) at a depth of 0.5 mm from the skin. It can be seen from Figure 6 that up to a distance of 1.5 mm from indenter, decreasing the radius of curvature (decreasing the indenter diameter) at the point of contact causes e_1 to increase as well. In the second set, the indenter was given a displacement as shown in Figure 5. The displacement reached a level of 1mm at time 0.1s , remained in the same place for 0.4s and decreased to zero in 0.1s . Thus the total indentation time is 0.6s . Figure 6 shows the variation of strain energy density as a function of time at different depths of 0 , 0.5 and 0.75mm from the skin exactly under the indenter. It can be seen that strain energy density increases rapidly to its maximum value at $t = 1\text{s}$, then decreases gradually and finally drops to zero at $t = 0.6\text{s}$.

Discussion and conclusion

The biomechanical properties of the skin and the subcutaneous tissues influence the transmission of mechanical vibration at different frequencies. As a result,

knowing the behavior of skin when it is subjected to different loads, is important in understanding the processes which involve tactile sensing such as minimally invasive surgery and designing tactile displays.

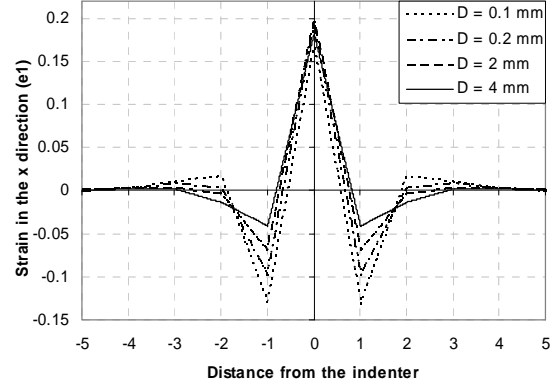


Figure 6: Vertical strain variations in the fingertip at a depth of 0.5mm from the skin surface plotted as a function of distance from the indenter.

In this study, we have proposed a finite element model to predict the response of fingertip subjected to a tactile stimulus. As most of the tactile displays are composed of arrays of vibrating pins, we have modeled the process of indentation of a typical pin as it interacts with the skin. If the skin on the fingerpad formed an infinite flat surface, then it would be sufficient to characterize the responses of afferents terminating in the region of the stimulus. However, the finger is a closed viscoelastic body with a curved surface. Bisley et al. [19] have found that mechanoreceptors located at sides of the fingertip react to the stimuli at the center of the fingertip. This is consistent with the results obtained from our model and plotted in Figure 3 which shows that the areas that are away from the indenter are also experiencing considerable amount of shear strain. Other quantities such as strain energy density also showed the same behavior (Figure 7).

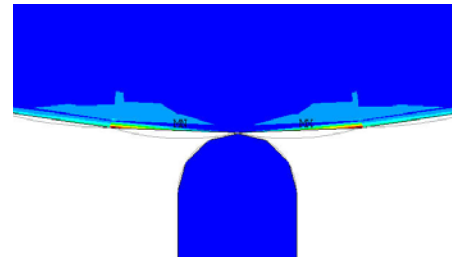


Figure 7: strain energy density distribution in the vicinity of indenter.

It is mentioned that mechanoreceptors in the human finger sense the vibrations in the range $5\text{-}250 \text{ Hz}$. Figure 8 shows the variation of strain energy density at different depths from the skin surface as a function of time in an indentation test where the indenter was given a

displacement as shown in Figure 8. It is seen that when the indenter is stationary during $t=0.1$ to $t=0.5$, the strain energy density decreases.

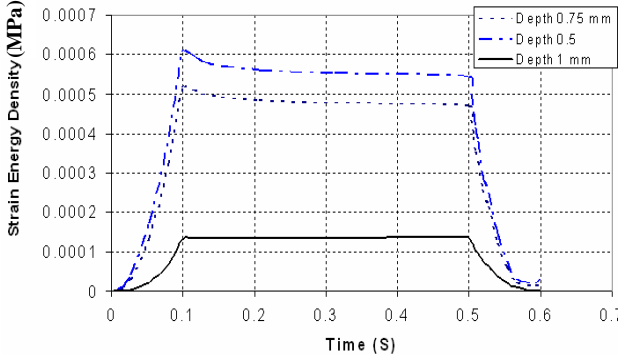


Figure 8: Strain energy density as a function of time for points located at depths of 0.5, 0.75, 1 mm from the skin.

Since the mechanoreceptors in the human finger can not sense the strain energy below a certain value, the frequency of indenter displacement can not be reduced greatly, otherwise the mechanoreceptors will be adapted. This adaptation causes the output of these receptors to become zero and the stimuli could not be felt.

Contrary to visual and auditory senses, the touch signal is not a well defined quantity. As a result, the researchers of this area are still dealing with the basics of collecting the most relevant data [19]. The mechanical parameter that the receptors in the finger perceive is still unknown and research in this area is in progress. By comparing the finite element results obtained using our model with experimental results, we can conclude that various strain-dependent parameters such as vertical strain, shear strain and strain energy density are appropriate candidates for the parameter that the mechanoreceptors perceive.

We have not included the effect of inertia on the response of fingertip. Future research could be concentrated on including these effects.

Appendix A. Constitutive equation for the skin

The skin is assumed to experience large deformation and possess nonlinearly elastic and linearly viscoelastic properties. The total tissue stress ($\tilde{\sigma}$) is assumed to be composed of elastic ($\tilde{\sigma}^0$) and viscous ($\tilde{\sigma}^v$) stress components, such that:

$$\begin{aligned} \tilde{\sigma}(t) &= \tilde{\sigma}^0(t) + \tilde{\sigma}^v(t) = \tilde{\sigma}^0(t) + \int_0^t \frac{\dot{G}^0(t)}{G_0} \tilde{\sigma}^0(t-\tau) d\tau \\ &= \tilde{\sigma}^0(t) + \int_0^t \dot{g}(\tau) \tilde{\sigma}^0(t-\tau) d\tau \end{aligned} \quad (1)$$

where t is time. Here the deformation behavior during the volumetric relaxation is considered to be identical to that attained under shear relaxation. The stress relaxation function is defined using the Prony series

$$g(t) = \frac{G(t)}{G_0} = \left[1 - \sum_{i=1}^{N_G} g_i (1 - e^{-t/\tau_i}) \right] \quad (2)$$

where G_0 and $G(t)$ are the instantaneous and time dependent moduli, respectively; g_i and τ_i ($i=1,2,\dots,N_G$) are stress relaxation parameters; N_G is the number of terms used in the stress relaxation function. The elastic deformation behavior of the soft tissue, based on finite deformation theory, is assumed to be nonlinearly elastic (hyperelastic). A function of strain energy density per unit volume, U , defined for the elastometric foams [28] is applied to describe the elastic behavior of the tissue in the following manner:

$$U = \sum_{i=1}^N \frac{2\mu_i}{\alpha_i^2} \left[\lambda_1^{\alpha_i} + \lambda_2^{\alpha_i} + \lambda_3^{\alpha_i} - 3 + \frac{1}{\beta} (J^{-\alpha_i \beta} - 1) \right] \quad (3)$$

where $J = \lambda_1 \lambda_2 \lambda_3$ is the volume ratio, λ_i ($i=1,2,3$) are the principal stretch ratios, α_i and μ_i ($i=1,2,\dots,N$) are the material parameters, $\beta = \nu / (1 - 2\nu)$ where ν is the Poisson's ratio, and N is the number of terms used in the strain energy function.

The elastic stress $\tilde{\sigma}^0$ is related to the elastic strain energy function (3) by:

$$\tilde{\sigma}^0 = \frac{2}{J} \tilde{F} \frac{\partial U}{\partial \tilde{C}} \tilde{F}^T \quad (4)$$

where \tilde{F} and \tilde{C} are the deformation gradient and the right Cauchy-Green deformation tensors, respectively.

Appendix B. Material properties of skin

Table 1: Material properties of skin

| i | 1 | 2 | 3 |
|---|-------------------------|------------------------|------------------------|
| Material parameters characterizing hyperelasticity for the skin ($\nu = .4$) | | | |
| α_i | 4.941 | 6.425 | 4.712 |
| μ_i (MPa) | -7.594×10^{-2} | 1.138×10^{-2} | 6.572×10^{-2} |
| Material parameters characterizing the hyperelasticity for the subcutaneous tissue ($\nu = .4$) | | | |
| α_i | 5.511 | 6.571 | 5.262 |
| μ_i (MPa) | -4.895×10^{-2} | 9.889×10^{-3} | 3.964×10^{-2} |
| Material parameters characterizing viscoelasticity for the skin ($\nu = .4$) | | | |
| g_i | 0.148 | 0.252 | - |
| τ_i (s) | 2.123 | 9.371 | - |

Acknowledgments

The authors are grateful to Eng. Seyed Mohsen Hosseini and Eng. Darbemamieh from Biomedical Engineering of Amirkabir University of Technology for providing valuable help and support.

References

- [1] Knibestol, M., 1973, "Stimulus-response functions of rapidly adapting mechanoreceptors in the human glabrous skin area", *J Physiol (Lond)*, **232**, 427–452.
- [2] Talbot W.H., Darian-Smith, I., Kornhuber, H.H., and Mountcastle, V.B., 1968, "The sense of flutter-vibration: comparison of the human capacity with response patterns of mechanoreceptive afferents from the monkey hand", *J Neurophysiol*, **31**, 301–334.
- [3] Johansson R.S., 1978, "Tactile sensibility in the human hand: receptive field characteristics of mechanoreceptive units in the glabrous skin area", *J Physiol (Lond)*, **281**, 101–123.
- [4] Phillips, J.R., and Johnson, K.O., 1981, "Tactile spatial resolution. II. Neural representation of bars, edges, and gratings in monkey primary afferents", *J Neurophysiol*, **46**, 1192–1203.
- [5] Pubols, B.H. JR., 1987, "Effects of mechanical stimulus spread across glabrous skin of raccoon and squirrel monkey hand on tactile primary afferent fiber discharge", *Somatosens Res*, **4**, 272–308.
- [6] Vega-Bermudez, F., and Johnson, K.O., 1999, "SA1 and RA receptive fields, response variability, and population responses mapped with a probe array", *J Neurophysiol*, **81**, 2701–2710.
- [7] Vega-Bermudez, F., and Johnson, K.O., 1999, "Surround suppression in the responses of primate SA1 and RA mechanoreceptive afferents mapped with a probe array", *J Neurophysiol*, **81**, 2711–2719.
- [8] Darian-Smith, I., 1984, "The sense of touch: performance and peripheral neural processes", In: *Handbook of Physiology—The Nervous System III*, edited by Brookhart JM, Mountcastle VB, Darian-Smith I, and Geiger SR. Bethesda, MD: *American Physiological Society*, 739–788.
- [9] Vallbo, A.B., 1995, "Single-afferent neurons and somatic sensation in humans", In: *The Cognitive Neurosciences*, edited by Gazzaniga, M.S., Cambridge, MA: MIT Press, 237–252.
- [10] Ikei, Y., Yamada, M., Fukuda, S., 2001, "A new design of haptic texture display-texture display 2- and its preliminary evaluation", IEEE, 21–28.
- [11] Kaczmarek, K., Bach-Y-Rita, P., Tompkins, W.J. and Webster, J.G., 1985, "A tactile vision-substitution system for the blind: computer-controlled partial image sequencing", *IEEE Transaction on Biomedical Engineering*, **8**, 602–608.
- [12] Ikei, Y., Fukuda, S., 1997, "Tactile display for a surface texture sensation", Proceeding of ASME Design Engineering Technical Conferences, 1–8.
- [13] Ikei, Y., Yamada, M., Fukuda, S., 1997-8, "Tactile display for tactile sensation", Proceedings of 7th International Conference on Human-Computer Interaction, 961–964.
- [14] Najarian, S., Dargahi, J. and Zheng, X.Z. (2006), "A novel method in measuring the stiffness of sensed objects with applications for biomedical robotic systems", *International Journal of Medical Robotics and Computer Assisted Surgery*, **2**, 84-90.
- [15] Bisley, J., W., Goodwin, A., W., 2000, "Slowly adapting type I afferents from the sides and end of the finger respond to stimuli on the center of the fingerpad", *Journal of Neurophysiology*, **84**, 57-64
- [16] Srinivasan, M. A., 1989, "Surface deflection of primate fingertip under line load", *Journal of Biomechanics*, **22**, 343-349.
- [17] Yamada, H., 1970, "Strength of biological materials", *Baltimore: Williams and Wilkins Co.*
- [18] Zheng Y, Mak A., 1996, "An ultrasound indentation system for biomechanical properties assessment of soft tissues in-vivo", *IEEE Biomed Eng*, **43**, 912–8.
- [19] Dargahi, J., Najarian, S., 2004, "Human tactile perception as a standard for artificial tactile sensing—a review", *Medical Robotics and Computer Assisted Surgery*, **1**, 23-35.